JOURNAL OF BACTERIOLOGY, May 2005, p. 3013–3019 Vol. 187, No. 9
0021-9193/05/$08.00+0 doi:10.1128/JB.187.9.3013–3019.2005

Requirements for *Vibrio cholerae* HapR Binding and Transcriptional Repression at the *hapR* Promoter Are Distinct from Those at the *aphA* Promoter

Wei Lin, Gabriela Kovacikova, and Karen Skorupski*

Department of Microbiology and Immunology, Dartmouth Medical School, Hanover, New Hampshire 03755

Received 1 December 2004/Accepted 31 January 2005

Virulence gene expression in certain strains of *Vibrio cholerae* is regulated in response to cell density by a quorum-sensing cascade that influences the levels of the LuxR homolog HapR through small regulatory RNAs that control the stability of its message. At high cell density, HapR represses the expression of the gene encoding the virulence gene activator AphA by binding to a site between −85 and −58 in the *aphA* promoter. We show here that a second binding site for HapR lies within the *hapR* promoter from which it functions to repress its own transcription. This site, as determined by gel mobility shift assay and DNaseI footprinting, is located between +8 and +36 from the transcriptional start and is not strongly conserved with the site at the *aphA* promoter. At low cell density, when the expression of a transcriptional *hapR-lacZ* fusion was low, no autorepression was observed. However, at high cell density, when the expression of the *hapR-lacZ* fusion was approximately 15-fold higher, the presence of HapR reduced its expression. Introduction of a single base pair change within the binding site at +18 prevented HapR binding in gel mobility shift assays. In the absence of HapR, this mutation did not significantly influence the expression of the *hapR* promoter, but in its presence, the expression of the promoter was increased at high cell density. These results indicate that HapR autorepresses from a single binding site in the *hapR* promoter and suggest a model for the temporal regulation of its expression as its intracellular levels increase.

Cholera is an often fatal epidemic diarrheal disease caused by oral ingestion of food or water contaminated with the bacterium *Vibrio cholerae*. The two primary virulence factors responsible for the disease are the toxin coregulated pilus (TCP), a critical colonization factor (24), and cholera toxin, which causes copious diarrhea that can quickly lead to severe dehydration and death. The expression of these genes from the *Vibrio* pathogenicity island (10) and the lysogenic cholera toxin phage (25), respectively, is dependent upon a transcriptional cascade involving multiple activator and repressor proteins (4) that is initiated at the *tcpPH* promoter by the regulators AphA and AphB (11, 23).

AphA is a member of a new transcriptional regulator family that shows homology to PadR, a repressor that controls the expression of genes involved in the detoxification of phenolic acids (1). Recent crystal structure determination of AphA revealed that it is a winged helix DNA binding protein with a unique antiparallel coiled coil domain that is involved in dimerization (5). AphA activates the transcription of the *tcpPH* promoter on the *Vibrio* pathogenicity island by an unusual mechanism that appears to require a direct interaction with the LysR-type regulator AphB, which binds at an adjacent and proximal site in the promoter (15). This interaction stabilizes the binding of AphB to its recognition site thereby facilitating transcriptional activation under the appropriate environmental conditions.

The expression of AphA in *V. cholerae* is regulated by a quorum-sensing system that responds to cell density (19, 26). At low cell density, AphA levels are relatively high and virulence gene activation ensues. However, as the cell density increases, HapR, which is a LuxR homolog, binds to a specific site in the *aphA* promoter that represses its expression (13). This, in turn, reduces virulence gene expression. HapR was initially characterized as an activator of hemagglutinin (HA)/protease in *V. cholerae* (9) and has recently been shown to play a role in repressing biofilm formation (7, 27). Its expression in *V. cholerae* is dependent upon several quorum-sensing circuits that function in parallel (19, 26). System 1 is composed of the CqsA-dependent autoinducer CAI-1 and its sensor CqsS. System 2 is composed of the LuxS-dependent autoinducer AI-2 and its sensor LuxPQ. It appears that a third quorum-sensing system, not yet identified, also contributes to this process.

The quorum-sensing circuits function together to control the activity of the central response regulator LuxO (17, 19). According to the current model, at low cell density, when the concentrations of autoinducers are low, LuxO is phosphorylated by a relay from the sensor proteins. This activated form of LuxO, in association with σ^{54}, activates the expression of several small regulatory RNAs (sRNAs) that in conjunction with the RNA binding protein Hfq destabilize the *hapR* message (16), thus permitting high-level expression of the virulence cascade. At high cell density, binding of autoinducers to their cognate sensors leads to dephosphorylation of LuxO. LuxO no longer activates the expression of the sRNAs. This increases *hapR* message stability and HapR, in turn, functions to downregulate expression of the virulence cascade by repressing expression from the *aphA* promoter.

The related marine organism *Vibrio harveyi* has a quorum-sensing circuit similar to that of *V. cholerae* in which LuxO

* Corresponding author. Mailing address: Department of Microbiology and Immunology, Dartmouth Medical School, Hanover, NH 03755. Phone: (603) 650-1623. Fax: (603) 650-1318. E-mail: karen.skorupski@dartmouth.edu.

TABLE 1. Bacterial strains and expression plasmids used in this study

Strain or plasmid	Relevant genotype	Reference or source
V. cholerae strain		
C6706 str2	E1 Tor Inaba Sm^r	Laboratory collection
KSK262	C6706 str2 Δ*lacZ3*	11
GK972	KSK262 Δ*hapR-lacZ*	This work
KSK2226	KSK262 $hapR^+$ *lacZ*::*hapR-lacZ*	This work
KSK2234	KSK2226 Δ*hapR*	This work
KSK2316	KSK262 Δ*hapR-lacZ* +18 A to G	This work
KSK2337	KSK262 $hapR^+$ *lacZ*::*hapR-lacZ* +18 A to G	This work
KSK2339	C6706 +18 A to G in *hapR* promoter	This work
Expression plasmids		
pKAS189	pMMB66EH *hapR*	13

controls the expression of bioluminescence in response to cell density (8, 16, 19). At high cell density, the *V. harveyi* LuxR protein functions to activate the *lux* promoter (20), and it also autorepresses its expression by binding to several sites in its own promoter (2). The parallels between HapR in *V. cholerae* and LuxR in *V. harveyi* prompted us to determine whether HapR also binds to its own promoter and similarly functions in autorepression. By constructing *hapR-lacZ* transcriptional fusion strains we show here that HapR is capable of reducing its own expression at high cell density. Gel mobility shift assays and DNaseI footprinting with purified HapR indicate that the protein recognizes a binding site downstream of its own promoter that extends from +8 to +36 relative to the start of transcription, consistent with a role in autorepression. To confirm that HapR binding to this site results in autorepression, a single A-to-G mutation was introduced into the site at +18. This mutation prevented HapR from binding in vitro in gel mobility shift assays and eliminated autorepression in vivo. Since the recognition sequence of the site at the *hapR* promoter is only weakly conserved with that at the *aphA* promoter and appears to have a lower binding affinity, this suggests these promoters are temporally regulated by HapR as its intracellular levels increase.

MATERIALS AND METHODS

Bacterial strains and expression plasmids. The *V. cholerae* strains and expression plasmids used in this study are listed in Table 1. Strains were maintained at −70°C in Luria-Bertani (LB) medium (18) containing 30% (vol/vol) glycerol. Antibiotics were used at the following concentrations in LB medium: ampicillin, 100 μg/ml; kanamycin, 45 μg/ml; polymyxin B, 50 units/ml; streptomycin, 1 mg/ml. 5-Bromo-4-chloro-3-indolyl-β-D-galactopyranoside (X-Gal) was used in LB agar at 40 μg/ml.

Construction of *hapR-lacZ* chromosomal fusions. A Δ*hapR* plasmid, pKAS187, was previously constructed which contains two 500-bp fragments of DNA that flank the *hapR* gene joined at a NotI restriction site (13). The *V. cholerae* Δ*hapR-lacZ* fusion was constructed by digesting this plasmid with NotI and inserting a promoterless *lacZ* gene from pVC200 (21) that has its own ribosome binding site and ATG codon, generating pGKK273. The resulting fusion was then introduced into the chromosome of KSK262 by allelic exchange, simultaneously creating a deletion of the *hapR* gene and a fusion of the *hapR* promoter to *lacZ* in the resulting strain, GK972. The merodiploid $hapR^+$ *hapR-lacZ* fusion was constructed as follows. A fragment from pGKK273 containing the *hapR-lacZ* fusion was obtained using an EcoRI site 500 bp upstream of the *hapR* gene and a BglII site which lies immediately downstream of *lacZ* and it was ligated into pKAS180 which contains two 500-bp fragments flanking the *V. cholerae lacZ* gene (14). The resulting fusion in pKAS264 was then introduced in place of the *lacZ* gene in KSK262, generating strain KSK2226. The Δ*hapR* mutation was then introduced with pKAS187 (13). The *hapR* overexpression plasmid pKAS189 (13) contains the *hapR* coding sequence expressed from a heterologous promoter in pMMB66EH.

Construction of *hapR* promoter mutations. The base pair changes in the *hapR* promoter were constructed by overlapping PCR using primers which contain the site for the type IIS restriction enzyme EarI. For each change, two 500-bp products were amplified from C6706 and then ligated into pKAS154 (13). The mutant products were amplified using primers HA24 (+18) (5′-GATCGCTCT TCGATTCTGTTATTTGCTACTTAAAGCCC), HA23 (+21) (5′-GATCGCT CTTCGATTTTGCTATTTGCTACTTAAAGCCCTATG), or HA25 (+18 and +21) (5′-GATCGCTCTTCGATTCTGCTATTTGCTACTTAAAGCCCTATG) together with primer HA16 (5′-GATCGGAATTCGTTTAAGGTATTCCCTG TATCG). The wild-type product was generated using primers HA22 (5′-GATC GCTCTTCGAATAATCATTAGAGCAAAATGC) and HA17 (5′-GATCGTC TAGAGCAGTTGGTTAGTTCGGTTG). After ligation, the resulting plasmids were sequenced. One of these, pWEL85, was used to introduce the +18 mutation into C6706 by allelic exchange to generate KSK2339. To construct the Δ*hapR-lacZ* chromosomal fusion containing the +18 change, an EcoRI NotI fragment containing the mutation was removed from pWEL85 and used to replace the wild-type fragment in pKAS187 described above. The promoterless *lacZ* gene described above was then inserted into the plasmid, generating pKAS275. After sequencing, the fusion was introduced into KSK262 by allelic exchange, generating KSK2316. To construct the merodiploid $hapR^+$ *hapR-lacZ* chromosomal fusion containing the +18 change, the EcoRI BglII *hapR* promoter-*lacZ* fragment analogous to that isolated from pGKK273 above was digested out of pKAS275 and ligated into pKAS180 (14). The resulting fusion in pKAS282 was then introduced in place of the *lacZ* gene in KSK262, generating KSK2337.

Identification of the *hapR* transcriptional start site. Total RNA was isolated from C6706 after growth for 7.5 h in LB medium at 37°C with TRIZOL reagent (Invitrogen). The RNA was subjected to 5′ rapid amplification of cDNA ends (Invitrogen) as described previously (14), except that first-strand cDNA synthesis was carried out using the *hapR*-specific primer HA11 (5′-CTTCTTGTTCACC TAAACGG) and the first and second nested primers were HA12 (5′-GTTGG GTGTGCGGTTGGTTG) and HA13 (5′-CAAACCACTCACCTAAAGCG).

Purification of HapR. HapR was purified using the IMPACT-CN protein fusion and purification system (New England Biolabs). The HapR gene was amplified from C6706 using HA-Sap (5′-GATCGGCTCTTCAGCACGCGTTC TTATAGATACACAGCA) and HA-Nde (5′-GATCGCATATGGACGCATC AATCGAAAAACG). The resulting fragment was digested with NdeI and SapI and ligated into pTXB-1 to generate pWEL20. The nucleotide sequence was confirmed by DNA sequencing. *Escherichia coli* strain ER2566 containing pWEL20 was grown in LB Amp at 30°C for 3 h, induced with 1 mM IPTG (isopropyl-β-D-thiogalactopyranoside) and shifted to 12°C, and growth was continued overnight. The cells were collected by centrifugation and resuspended in column buffer (20 mM Tris [pH 8.0], 500 mM NaCl, 1 mM EDTA). The extract was sonicated and clarified by centrifugation at 14,000 rpm for 30 min in an SS34 rotor. The supernatant was then loaded onto a chitin column equilibrated with column buffer and washed with 10 volumes of column buffer and high-salt column buffer (containing 1 M NaCl). The column was then quickly washed with 3 volumes of cleavage buffer (column buffer containing 100 mM dithiothreitol [DTT]) and was left overnight at 16°C. HapR was then eluted off the column by using column buffer without DTT. The resulting protein was dialyzed overnight in a solution of 20 mM Tris (pH 7.5), 1 mM EDTA, 10 mM NaCl, and 0.1 mM DTT, glycerol was added to 10%, and it was frozen at −70°C. The final purity was estimated to be greater than 98%.

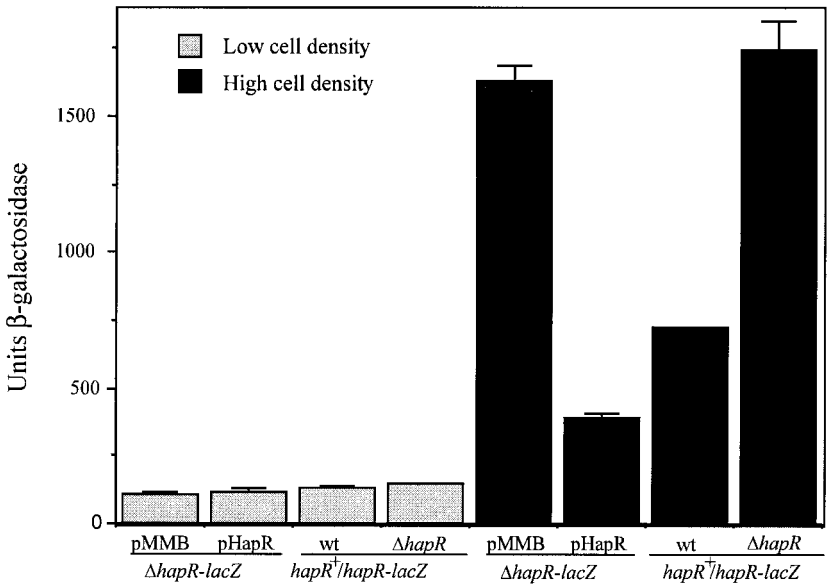

FIG. 1. Influence of HapR on *hapR-lacZ* fusions in *V. cholerae*. Strains were grown in LB medium at 37°C for 2 h (low cell density, OD_{600} = 0.2) or 8 h (high cell density, OD_{600} = 4.0). From left to right: GK972 (Δ*hapR-lacZ*) pMMB66EH (vector control), GK972 pKAS189 (pMMB66EH/*hapR*$^+$), KSK2226 (*hapR*$^+$/*hapR-lacZ*), KSK2234 (KSK2226 Δ*hapR*). Cultures with pMMB66EH and pKAS189 contained 1 mM IPTG. wt, wild type.

Gel mobility shift experiments. A 150-bp *hapR* promoter fragment was amplified by PCR from C6706 or the *E. coli* strains containing the mutant plasmids pWEL84 (+21G), pWEL85 (+18G), or pWEL86 (+18G, +21G) using primers HA4 (−61) (5′-GATCGGAATTCGTTGCACATTTTTCACCCAAC) and HAN1 (+96) (5′-GATCGGCGGCCGCTTCGATTGATGCGTCCATAG). A 120-bp *hapR* promoter fragment was amplified from C6706 using primers HA5 (+41) (5′-TGCTCAATCAACAACTCAATTG) and HA6 (+158) (5′-GATCG GGATCCAACGCGATTTCCATCAGTTG). The fragments were gel purified, 3′ end labeled with digoxigenin and visualized using chemiluminescence (12). Binding reactions for HapR were carried out as previously described (13).

DNaseI footprinting. A 350-bp fragment was PCR amplified from C6706 with HA3E (−198) (5′-GATCGGAATTCGCGATGTCAGTATCGCTGAC) and HA6 (+158) and ligated into pBluescript (Stratagene), generating pWEL81. For upper-strand labeling, the inserts were excised with EcoRI and XbaI. For lower-strand labeling, the inserts were excised with BamHI and HindIII. The fragments were gel purified, treated with shrimp alkaline phosphatase, and kinased with [γ-^{33}P]ATP (NEN; 3,000 Ci/mmol). Singly end-labeled fragments were obtained by digestion with BamHI (for the upper strand) and EcoRI (for the lower strand). Proteins were bound to the singly end-labeled DNA fragment as previously described (13).

Real-time quantitative reverse transcription (RT)-PCR. Overnight cultures of C6706 and KSK2339 were incubated in LB medium at 30°C with shaking. The cultures were diluted 1:00 into fresh LB medium and incubated at 37°C until the optical density at 600 nm (OD_{600}) reached 0.5. They were then diluted 1:5 and growth was continued until the OD_{600} reached 2.0. The cells were collected by centrifugation and RNA was isolated using TRIZOL (Invitrogen). The RNA was subjected to DNaseI and purified using RNeasy columns (QIAGEN). Equal amounts of RNA (5 μg) were used to generate cDNA (Invitrogen). To ensure that the RNA preparations were free from genomic DNA, reverse transcription was performed with or without reverse transcriptase. Quantitative PCR was carried out by performing two independent experiments each in triplicate with 20 ng of cDNA using QuantiTect SYBR Green master mix (QIAGEN). PCR was monitored using the ABI Prism 7700 detection system. The primers for *hapR* were HapRF (5′-AACTGATGGAAATCGCGTTG) and HapRR (5′-AACAC TGTTGCAACGGAGAC), which generated a 100-bp product. Primers for the gene encoding ribosomal protein L27 (*rpmA*) which served as the endogenous control were RpmF (5′-AGCTGGTGGTTCTACTCGTAACG) and RpmR (5′-CGAACGATGATGTTACCTGC), which generated a 101-bp product. Relative *hapR* expression was determined using the following calculation: $2^{-(\Delta C_T}$ target − ΔC_T control), where C_T is the threshold cycle. The levels of *rpmA* were essentially identical in the strains examined.

β-Galactosidase assays. Assays with *V. cholerae lacZ* fusions were carried out as described previously (18).

RESULTS

HapR influences the transcription of the *hapR* promoter in *V. cholerae*. To determine whether the *V. cholerae* HapR protein functions similarly to LuxR as an autorepressor, a Δ*hapR-lacZ* transcriptional fusion strain, GK972, was constructed. In this strain, the *hapR* coding sequence was replaced with an *E. coli lacZ* gene containing its own ribosome binding site and ATG codon, thus rendering its expression independent of translational regulation through LuxO. A plasmid overexpressing HapR from a heterologous promoter, pKAS189, was then introduced into GK972. Although at low cell density (OD_{600} = 0.2) no significant difference in expression was observed compared to a vector control (Fig. 1), at high cell density (OD_{600} = 4.0) the expression of the fusion increased approximately 15-fold over that at low cell density, and under this condition the presence of HapR from pKAS189 resulted in a fourfold reduction in β-galactosidase activity (Fig. 1). To determine if a similar effect also occurs when *hapR* is in single copy, a *hapR*$^+$ merodiploid strain was constructed by introducing the *hapR-lacZ* reporter into the *lacZ* locus by homologous recombination with regions of the flanking *chrA* and *galR* genes (14). The resulting strain, KSK2226, harbors the same *hapR* promoter-*lacZ* fusion as in GK972, but it is situated at the *lacZ* locus, leaving the *hapR* gene intact at its normal chromosomal location. KSK2226 was then compared with an isogenic strain containing a Δ*hapR* mutation. Again, at low cell density no significant difference between the strains was observed (Fig. 1), but at high cell density a twofold increase in expression was observed in the Δ*hapR* strain, consistent with a role for HapR in its negative autoregulation (Fig. 1).

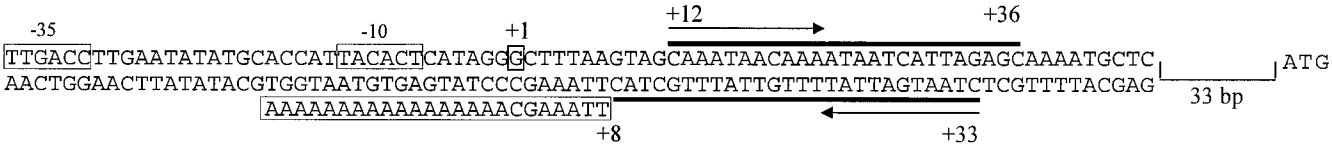

FIG. 2. Nucleotide sequence of the proximal region of the *hapR* promoter. The transcriptional start site (+1), ATG codon, and −10 and −35 regions are shown. Black lines show the region of the promoter protected by HapR, and arrows indicate putative dyad symmetry. The boxed sequence below the nucleotide sequence shows the data used to determine the position of the transcriptional start.

Identification of the *hapR* transcriptional start site. The transcriptional start site for the *hapR* promoter was determined using 5′ rapid amplification of cDNA ends (6) with RNA isolated from wild-type C6706 grown in LB medium at 37°C to high cell density. A product corresponding to the size expected for the transcriptional start was identified, and sequencing of it revealed that the +1 of the *hapR* promoter is a G 77 bp upstream of the ATG (Fig. 2). The −10 sequence, TACACT, shows two mismatches from the consensus TATAAT, and the −35 sequence, TTGACC, has only one mismatch from the consensus TTGACA.

HapR binds to a site in the *hapR* promoter downstream of the transcriptional start. Gel mobility shift assays were used to localize the HapR binding site in the *hapR* promoter. As shown in Fig. 3, a single shift was observed in the presence of increasing amounts of purified HapR protein on a DNA fragment encompassing the region from −61 to +96. However, no shift was observed on a fragment from +41 to +158, indicating that the HapR binding site is located between −61 and +41 in the promoter. No additional complexes with slower mobility were observed on a larger fragment extending upstream in the promoter to −116 (data not shown), indicating that HapR does not recognize any other sites in the promoter with a similar affinity.

To further localize the binding site between −61 and +41, DNaseI footprinting was utilized. On a 350-bp fragment extending from −198 to +158, a single site of strong protection was observed (Fig. 4). On the top strand, this site extended from +12 to +36, and on the bottom strand, it extended from +8 to +33 (Fig. 2). No other strong regions of protection were observed on this fragment, suggesting that a single site is necessary for HapR autorepression. Comparison of a 22-bp sequence of partial dyad symmetry within the footprint (Fig. 5A) to the site previously identified at the *aphA* promoter (13) reveals the lack of a strong HapR binding motif. Of the 10 bp which are conserved between the sites, six of these are symmetrical in both, indicating that there is a degree of functional similarity between them.

Identification of a point mutation in the HapR binding site that prevents binding. We have previously shown that a naturally occurring base pair change in classical biotype strains at position −77 from G to T in the HapR binding site at the *aphA*

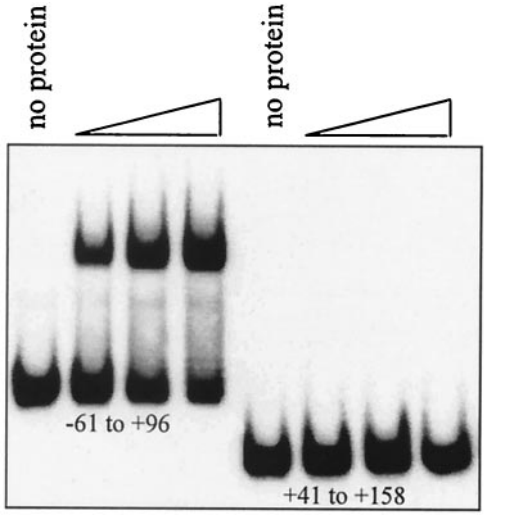

FIG. 3. Binding of purified HapR to specific *hapR* promoter fragments. Lanes 1–4, a 150-bp fragment from −61 to +96; lanes 5–8, a 120-bp fragment from +41 to +158. The first lane in each set has no protein added, the second lane has 36 nM (18 ng) HapR, the third lane has 70 nM (35 ng) HapR, and the fourth lane has 140 nM (70 ng) HapR.

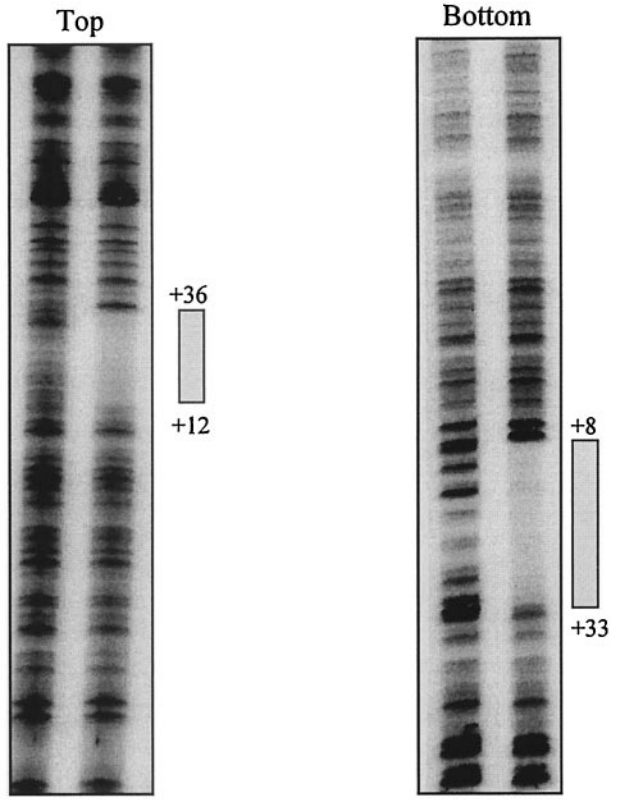

FIG. 4. DNaseI footprint for HapR at the *hapR* promoter. Top and bottom strands of a 350-bp fragment from −198 to +158. Lane 1, no protein; lane 2, 1.4 μM (176 ng) HapR.

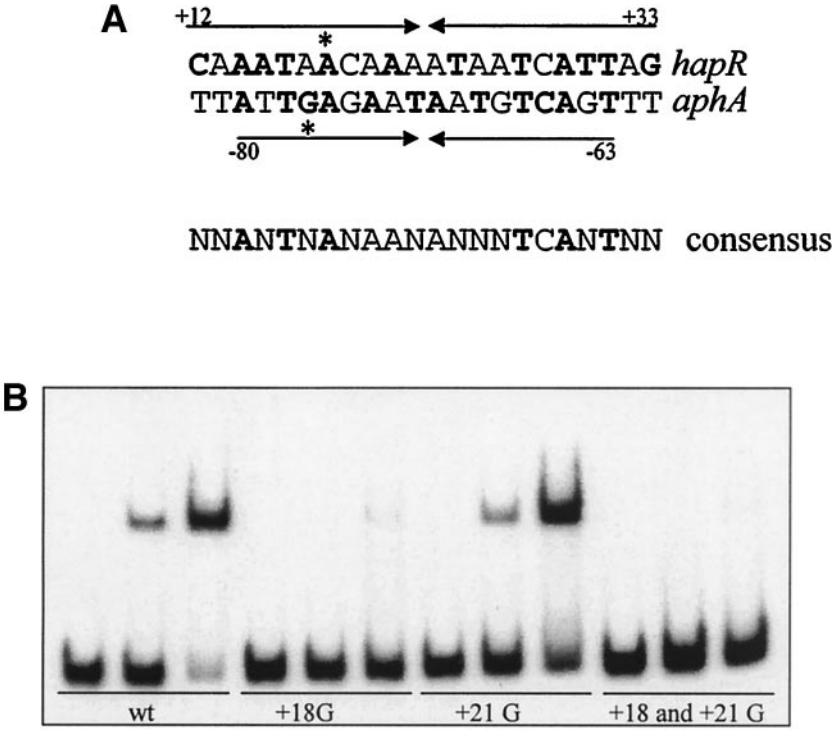

FIG. 5. A. Comparison of the HapR binding sites at the *hapR and aphA* promoters. Arrows show the extent of dyad symmetry and bold characters show positions that are symmetrical in each site. Asterisks denote positions where single base pair changes prevent HapR binding. B. Binding of purified HapR to the 150-bp fragment from −61 to +96. The first three lanes are wild type (wt), the next three lanes contain the +18 A-to-G mutation, the next three lanes contain the +21 A-to-G mutation, and the last three lanes contain both mutations. The first lane in each set has no protein added, the second lane has 36 nM (18 ng) HapR, and the third lane has 140 nM (70 ng) HapR.

promoter completely prevents HapR binding, indicating it is critical for its recognition (13). Since the analogous position in the HapR binding site at the *hapR* promoter (+17) is not conserved (Fig. 5A), nor does it appear to be important for symmetry, identification of a base pair change that prevents the protein from binding to the promoter was not straightforward. Therefore, two base pairs were changed to G that appeared to be important for maintaining the dyad symmetry of the site (A at position +18 and A at position +21). When these base pair changes were introduced into the −61 to +96 fragment which is capable of binding HapR (Fig. 3), the +18 change prevented binding whereas the +21 change did not (Fig. 5B). As expected from this, a fragment containing both mutations was also defective for binding (Fig. 5B). These results indicate that HapR binding at its own promoter can be disrupted by a single base pair change at position +18.

The G +18 mutation in the HapR binding site prevents autorepression. To determine if the +18 A-to-G change that interferes with HapR binding to its own promoter also prevents autorepression, its influence on *hapR-lacZ* fusions in Δ*hapR* and *hapR*$^+$ strains was determined. As shown in Fig. 6, the expression of the Δ*hapR-lacZ* fusion containing the G +18 mutation (KSK2316) was only slightly higher than that of the wild-type fusion GK972 at both low and high cell density, indicating that the point mutation does not significantly influence the expression of the *hapR* promoter in the absence of HapR. However, in the presence of HapR, the expression of the fusion containing the G +18 mutation (KSK2337) showed approximately twofold derepression at high cell density such that it appeared similar to the wild-type fusion lacking HapR. These results indicate that HapR autorepresses by binding to the site identified in the *hapR* promoter that extends from +8 to +36. Consistent with this, the level of *hapR* expression as determined by real-time RT-PCR in C6706 containing the +18 A-to-G change at high cell density was approximately twofold higher than in the wild type (Fig. 7).

DISCUSSION

In strains of *V. cholerae* with a functional HapR protein, quorum sensing plays an important role in influencing various cellular processes. At low cell density, *hapR* message is destabilized by sRNAs in conjunction with Hfq such that its levels are insufficient to significantly repress *aphA* and the expression of virulence genes or the expression of polysaccharide genes required for biofilm formation. As the cell density increases, *hapR* message becomes stabilized, and this leads to an accumulation of HapR which downregulates virulence and polysaccharide gene expression and activates HA protease expression. The work presented here sheds additional light on the control of *hapR* expression in *V. cholerae* by showing that HapR is capable of repressing its own transcription at high cell density. At low cell density, the expression of a transcriptional *hapR-lacZ* fusion is fairly low and regulation is primarily achieved at the level of translation (16). However, as the cell density increases, the stability of the *hapR* message increases as well as

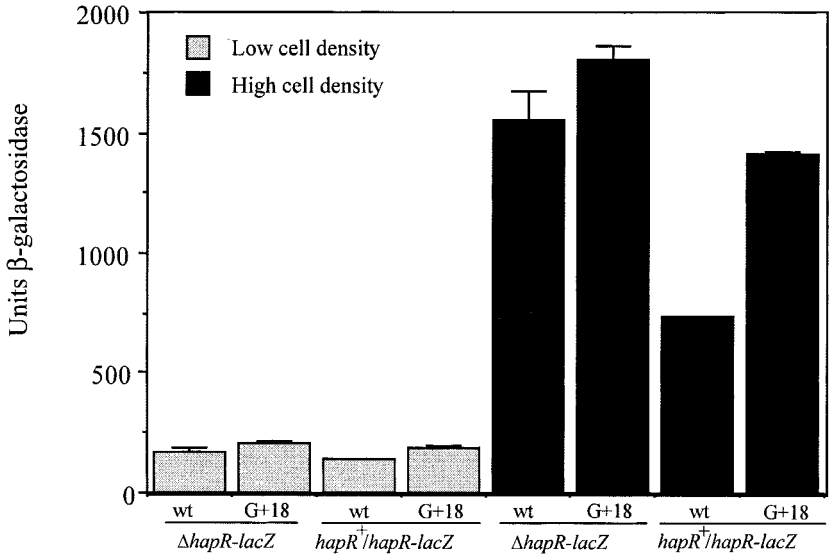

FIG. 6. Influence of the +18 A-to-G change on Δ*hapR* and *hapR*$^+$ *lacZ* fusions in *V. cholerae*. Strains were grown in LB medium at 37°C for 2 h (low cell density, OD_{600} = 0.2) or 8 h (high cell density, OD_{600} = 4.0). From left to right: GK972 (Δ*hapR-lacZ*), KSK2316 (Δ*hapR-lacZ* +18G), KSK2226 (*hapR*$^+$/*hapR-lacZ*), KSK2337 (*hapR*$^+$/*hapR-lacZ* +18G). wt, wild type.

its transcription, and HapR serves to downregulate this transcription through autorepression.

The location of the HapR binding site centered at +22 in the *hapR* promoter is consistent with its role as a transcriptional repressor. In gel shift and DNaseI footprinting experiments, HapR did not appear to bind strongly to any other sites in the promoter. This is in contrast to the *luxR* promoter, where LuxR was found to bind independently to two sites that contribute to autorepression: one around +25 similar to that at the HapR promoter and the other upstream of the transcriptional start between −107 and −52 (2). The finding that a single base pair change from A to G at +18 in the *hapR* promoter prevents HapR binding and virtually eliminates autorepression is consistent with the notion that HapR binding to this single site is responsible for this activity. Since LuxR appears to interfere with RNA polymerase binding (2), HapR likely functions by a similar mechanism.

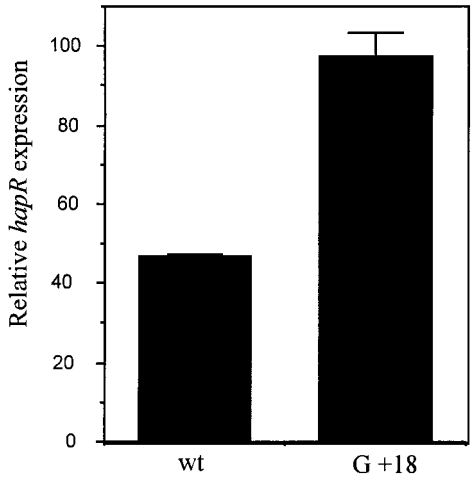

FIG. 7. Relative levels of *hapR* expression determined by real-time PCR. Cultures were grown in LB medium at 37°C to an OD_{600} of 2.0. RNA was isolated, converted to cDNA, and analyzed by real-time PCR. C6706 (wild type [wt]), KSK2339 (+18G).

HapR has previously been shown to bind to a recognition site at the *aphA* promoter from which it represses (13). The location of this site at −71 in the promoter raises the possibility that the protein employs different modes of action at the *hapR* and *aphA* promoters to repress transcription. It was somewhat surprising that the recognition sequences for HapR at the *aphA* and *hapR* promoters are only weakly conserved. The position in the *aphA* promoter that is critical for HapR binding (G at −77) is not conserved in the site at the *hapR* promoter nor does it contribute to its symmetry. Although the position in the *hapR* promoter that is critical for HapR binding and autorepression (A at +18) is conserved in the *aphA* promoter, it is not yet known whether this position is important for HapR binding to this site. Since it takes considerably less HapR protein to shift the site in the *aphA* promoter (13), it is likely that the affinity for the site in the *hapR* promoter is lower, such that HapR is only able to repress at high protein levels. In contrast, experiments have indicated that HapR is capable of binding to the *aphA* promoter and reducing its expression to some degree even at low cell density (13). Thus, the differences in the recognition sequences of HapR at the *aphA* and *hapR* promoters likely contribute to their different binding affinities, and this is important for the temporal regulation of these promoters as the intracellular levels of HapR increase.

Since HapR autorepression downregulates the transcription of the *hapR* promoter at high cell density, this suggests that autoregulation may serve to prevent runaway expression under this condition. It was somewhat unexpected that at low cell density the expression of the *hapR-lacZ* fusion was not also reduced in the presence of overexpressed HapR. One possibility is that the activity measured at low cell density is a background level derived by read-through from upstream of the promoter and therefore is not subject to regulation by

HapR. Alternatively, the levels of HapR from the overexpression plasmid after only 2 h of induction were insufficient to cause a reduction in the expression of the promoter.

Although the mechanisms involved in the transcriptional activation of the *hapR* and *luxR* promoters in *V. cholerae* and *V. harveyi* are not clearly understood, the cyclic AMP receptor protein appears to play a role in this process at both (3, 22). However, regulation by MetR appears to be different. In *V. harveyi*, MetR represses the *luxR* promoter (3), whereas a Δ*metR* mutation in *V. cholerae* does not appear to influence the expression of *hapR* (data not shown). It is not surprising that at least some of the factors influencing bioluminescence in *V. harveyi* and virulence/biofilm formation in *V. cholerae* are different. Further investigation into the regulation of these promoters will shed additional light on the mechanisms involved in these processes.

ACKNOWLEDGMENTS

We thank Ronald Taylor for critical reading of the manuscript.
This work was supported by NIH grant AI41558 to K.S.

REFERENCES

1. **Barthelmebs, L., B. Lecomte, C. Divies, and J.-F. Cavin.** 2000. Inducible metabolism of phenolic acids in *Pediococcus pentosaceus* is encoded by an autoregulated operon which involves a new class of negative transcriptional regulator. J. Bacteriol. **182:**6724–6731.
2. **Chatterjee, J., C. M. Miyamoto, and E. A. Meighen.** 1996. Autoregulation of *luxR*: the *Vibrio harveyi lux*-operon activator functions as a repressor. Mol. Microbiol. **20:**415–425.
3. **Chatterjee, J., C. M. Miyamoto, A. Zouzoulas, B. F. Lang, N. Skouris, and E. A. Meighen.** 2002. MetR and CRP bind to the *Vibrio harveyi lux* promoters and regulate luminescence. Mol. Microbiol. **46:**101–111.
4. **Cotter, P. A., and V. J. DiRita.** 2000. Bacterial virulence gene regulation: an evolutionary perspective. Annu. Rev. Microbiol. **54:**519–565.
5. **De Silva, R., G. Kovacikova, W. Lin, R. K. Taylor, K. Skorupski, and F. J. Kull.** Crystal structure of the virulence gene activator AphA from *Vibrio cholerae* reveals it is a novel member of the winged helix transcription factor superfamily. J. Biol. Chem., in press.
6. **Frohman, M. A., M. K. Dush, and G. R. Martin.** 1988. Rapid production of full-length cDNAs from rare transcripts: amplification using a single gene-specific oligonucleotide primer. Proc. Natl. Acad. Sci. USA **85:**8998–9002.
7. **Hammer, B. K., and B. L. Bassler.** 2003. Quorum sensing controls biofilm formation in *Vibrio cholerae*. Mol. Microbiol. **50:**101–114.
8. **Henke, J. M., and B. L. Bassler.** 2004. Three parallel quorum-sensing systems regulate gene expression in *Vibrio harveyi*. J. Bacteriol. **186:**6902–6914.
9. **Jobling, M. G., and R. K. Holmes.** 1997. Characterization of *hapR*, a positive regulator of the *Vibrio cholerae* HA/protease gene *hap*, and its identification as a functional homologue of the *Vibrio harveyi luxR* gene. Mol. Microbiol. **26:**1023–1034.
10. **Karaolis, D. K. R., J. A. Johnson, C. C. Bailey, E. C. Boedeker, J. B. Kaper, and P. R. Reeves.** 1998. A *Vibrio cholerae* pathogenicity island associated with epidemic and pandemic strains. Proc. Natl. Acad. Sci. USA **95:**3134–3139.
11. **Kovacikova, G., and K. Skorupski.** 1999. A *Vibrio cholerae* LysR homolog, AphB, cooperates with AphA at the *tcpPH* promoter to activate expression of the ToxR virulence cascade. J. Bacteriol. **181:**4250–4256.
12. **Kovacikova, G., and K. Skorupski.** 2001. Overlapping binding sites for the virulence gene regulators AphA, AphB and cAMP-CRP at the *Vibrio cholerae tcpPH* promoter. Mol. Microbiol. **41:**393–407.
13. **Kovacikova, G., and K. Skorupski.** 2002. Regulation of virulence gene expression in *Vibrio cholerae* by quorum sensing: HapR functions at the *aphA* promoter. Mol. Microbiol. **46:**1135–1147.
14. **Kovacikova, G., and K. Skorupski.** 2002. The alternative sigma factor σ^E plays an important role in intestinal survival and virulence in *Vibrio cholerae*. Infect. Immun. **70:**5355–5362.
15. **Kovacikova, G., W. Lin, and K. Skorupski.** 2004. *Vibrio cholerae* AphA uses a novel mechanism for virulence gene activation that involves interaction with the LysR-type regulator AphB at the *tcpPH* promoter. Mol. Microbiol. **53:**129–142.
16. **Lenz, D. H., K. C. Mok, B. N. Lilley, R. V. Kulkarni, N. S. Wingreen, and B. L. Bassler.** 2004. The small RNA chaperone Hfq and multiple small RNAs control quorum sensing in *Vibrio harveyi* and *Vibrio cholerae*. Cell **118:**69–82.
17. **Lilley, B. N., and B. L. Bassler.** 2000. Regulation of quorum sensing in *Vibrio harveyi* by LuxO and Sigma-54. Mol. Microbiol. **36:**940–954.
18. **Miller, J. H.** 1972. Experiments in molecular genetics. Cold Spring Harbor Laboratory, Cold Spring Harbor, N.Y.
19. **Miller, M. B., K. Skorupski, D. H. Lenz, R. K. Taylor, and B. L. Bassler.** 2002. Parallel quorum sensing systems converge to regulate virulence in *Vibrio cholerae*. Cell **110:**303–314.
20. **Miyamoto, C. M., E. E. Smith, E. Swartzman, J.-G. Cao, A. F. Graham, and E. A. Meighen.** 1994. Proximal and distal sites bind LuxR independently and activate expression of the *Vibrio harveyi lux* operon. Mol. Microbiol. **14:**255–262.
21. **Parsot, C., and J. J. Mekalanos.** 1990. Expression of ToxR, the transcriptional activator of the virulence factors in *Vibrio cholerae*, is modulated by the heat shock response. Proc. Natl. Acad. Sci. USA **87:**9898–9902.
22. **Silva, A. J., and J. A. Benitez.** 2004. Transcriptional regulation of *Vibrio cholerae* hemagglutinin/protease by the cyclic AMP receptor protein and RpoS. J. Bacteriol. **186:**6374–6382.
23. **Skorupski, K., and R. K. Taylor.** 1999. A new level in the *Vibrio cholerae* ToxR virulence cascade: AphA is required for transcriptional activation of the *tcpPH* operon. Mol. Microbiol. **31:**763–771.
24. **Taylor, R. K., V. L. Miller, D. B. Furlong, and J. J. Mekalanos.** 1987. Use of *phoA* gene fusions to identify a pilus colonization factor coordinately regulated with cholera toxin. Proc. Natl. Acad. Sci. USA **84:**2833–2837.
25. **Waldor, M. K., and J. J. Mekalanos.** 1996. Lysogenic conversion by a filamentous phage encoding cholera toxin. Science **272:**1910–1914.
26. **Zhu, J., M. B. Miller, R. E. Vance, M. Dziejman, B. L. Bassler, and J. J. Mekalanos.** 2002. Quorum sensing regulators control virulence gene expression in *Vibrio cholerae*. Proc. Natl. Acad. Sci. USA **99:**3129–3134.
27. **Zhu, J., and J. J. Mekalanos.** 2003. Quorum sensing-dependent biofilms enhance colonization in *Vibrio cholerae*. Dev. Cell **5:**647–656.